Temperature-Dependent Crystalline–Amorphous Structures in Isotactic Polypropylene: Small-Angle X-ray Scattering Analysis of Edge-Bounded Two-Phase Systems

T. Albrecht* and G. Strobl

Fakultät für Physik, Universität Freiburg, Hermann-Herder-Strasse 3, D-79104 Freiburg, Federal Republic of Germany

Received January 26, 1995; Revised Manuscript Received May 8, 1995[⊗]

ABSTRACT: Small-angle X-ray scattering (SAXS) experiments on isothermally crystallized isotactic polypropylene (iPP) reveal a clear temperature dependence of the crystalline–amorphous structure over a broad range of temperatures below the crystallization temperature. This phenomenon is analyzed using SAXS combined with dilatometry. A new concept for the evaluation of SAXS data—the specific length of edges L_s—is used. It allows a quantitative interpretation of $g''(0)$, the second derivative of the electron density correlation function at $r = 0$. Using this parameter, a clear identification of the relevant physical process is possible. Whereas primary crystallization leads to the formation of laterally extended crystalline lamellae, subsequent cooling generates additional small crystallites in the amorphous regions. A model relating this mode of partial crystallization and melting to the special morphology of iPP—the cross-hatched structure—is suggested.

Introduction

Small-angle X-ray scattering (SAXS) is a common method for the investigation of mesoscopic two-phase systems. A well-known application of this technique in the field of polymer science is the investigation of the amorphous–crystalline structure in partially crystalline polymers. The prominent object of study was for a long-time polyethylene. The applied methods of data evaluation are based on the model of a one-dimensional stack of crystalline lamellae.[10,12] The formation of the more complicated "cross-hatched" structure in isotactic polypropylene was analyzed by electron microscopy.[1,6,7] Lotz and Wittmann explain the existence of this structure by a special mode of epitaxial crystallization.[4]

Small-angle X-ray scattering is particularly suited for in situ observations of the structure at different temperatures. Temperature-dependent structural changes can indeed be observed in crystallizable polymers. So far these changes in the mesoscopic structure—known as "partial melting"—were mainly studied on polyethylene.[13] This work concerns the partial melting in polypropylene, and it turned out that the behavior is quite different from polyethylene. Data analysis requires the use of a new general concept which allows the determination of additional structural features.

Theory of Small-Angle X-ray Scattering—Method of Data Analysis

Structural Parameters and the Correlation Function. In an isotropic system the scattered intensity $I(s)$ at small angles is related to the electron density correlation function $g(r)$ by

$$I(s) = \frac{1}{r_e^2 V}\frac{d\sigma}{d\Omega} = 4\pi \int_0^\infty dr\, r^2 \frac{\sin(2\pi sr)}{2\pi sr} g(r), \qquad s = \frac{2}{\lambda}\sin\frac{\theta}{2} \quad (1)$$

s and θ denote the scattering vector and the Bragg angle. $I(s)$ is obtained in absolute units (e/nm^3). The correlation function $g(r)$ is defined by the following average over the sample volume:

$$g(r) = \langle \delta\varrho(\vec{r}')\, \delta\varrho(\vec{r}' + \vec{r}) \rangle_{\vec{r}'} \quad (2)$$

whereby $\delta\varrho$ denotes the deviation of the electron density from the mean value

$$\delta\varrho(\vec{r}) = \varrho(\vec{r}) - \langle\varrho\rangle \quad (3)$$

The mesoscopic amorphous–crystalline structure of partially crystalline polymers is usually well described as a two-phase system; i.e., the density $\varrho(\vec{r})$ takes on only two values

$$\varrho(\vec{r}) = \begin{cases} \varrho_c & \text{if } \vec{r} \text{ is in the crystalline phase} \\ \varrho_a & \text{if } \vec{r} \text{ is in the amorphous phase} \end{cases} \quad (4)$$

The calculations which follow would have to be modified if there were smooth transition zones between the two phases. In the experiments described here the corresponding changes in the scattering intensity did not show up. Additional contributions to the scattered intensity due to density fluctuations within the individual phases are also disregarded; during the process of data evaluation, they were subtracted by empirical means.

The behavior of $g(r)$ in the vicinity of $r = 0$ is determined by main structural parameters of the two-phase system. A straightforward calculation gives without any further assumptions the well-known result

$$g(0) = \omega_c \omega_a \Delta\varrho^2 \quad (5)$$

with ω_c and ω_a denoting the volume fractions of crystalline and amorphous material. $\Delta\varrho$ is the difference $\varrho_c - \varrho_a$.

The value of $g'(0)$, the first derivative of the function $g(r)$ at $r = 0$, has a definite geometrical meaning, too. It is related to the amount of interface per volume, i.e., the "specific inner surface" O_s. Although this is a well-known fact,[8] a derivation is given here, because we will use a similar argument when considering the signifi-

[⊗] Abstract published in *Advance ACS Abstracts,* June 15, 1995.

0024-9297/95/2228-5267$09.00/0 © 1995 American Chemical Society

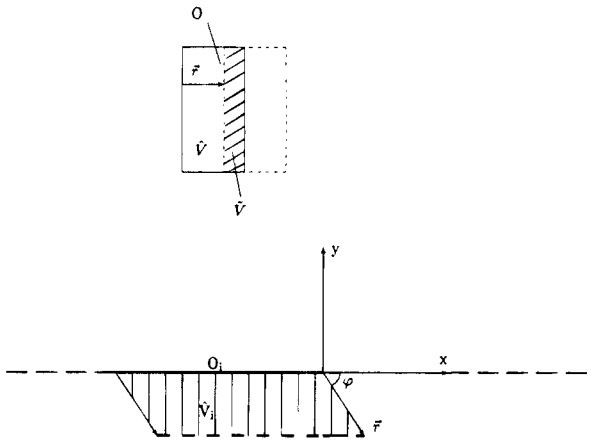

Figure 1. Geometrical procedure employed in the calculation of $\tilde{g}(r)$.

cance of the second derivative $g''(0)$. It is convenient to consider the function

$$\tilde{g}(r) = \langle(\varrho(\vec{r}') - \varrho_a)(\varrho(\vec{r}' + \vec{r}) - \varrho_a)\rangle \quad (6)$$

$$= g(r) + \omega_c^2 \Delta\varrho^2 \quad (7)$$

to which pairs of points, $\vec{r}'$ and $\vec{r}' + \vec{r}$, contribute only if they are both lying in the crystalline part of the sample. In order to see the geometrical meaning of this function, let us consider a crystalline particle surrounded by amorphous material. If we superpose the same particle, but shifted by a vector $\vec{r}$, on the original structure, all points contributing to the function $\tilde{g}(\vec{r})$ are contained in the volume $\hat{V}(\vec{r})$, common to the original and the shifted particle. Isotropic averaging then leads to the function $\tilde{g}(r)$. In the vicinity of $r = 0$, $\tilde{g}(r)$ can be decomposed into contributions due to pieces of interface O_i. An example is indicated in Figure 1. The volume $\hat{V}_i$, built up when the interface is shifted by a vector $\vec{r}$, determines the decrease of $\tilde{g}(r)$ associated with O_i. In order to obtain the total decrease, the contribution of all parts O_i have to be summed up

$$\tilde{g}(\vec{r}) = \tilde{g}(0) - \sum_i \frac{\hat{V}_i(\vec{r})}{V} \Delta\varrho^2 \quad (8)$$

V denotes the volume of the system. In a first-order approximation $\hat{V}_i$ can be written as the product

$$\hat{V}_i(\vec{r}) = O_i|\vec{r}| \sin\varphi \quad (9)$$

The angle φ is defined in Figure 3. Taking an isotropic average over all directions of the vector $\vec{r}$, we get as the final result

$$\tilde{g}(r) = \tilde{g}(0) - \frac{O_s}{4}\Delta\varrho^2 r \quad (10)$$

Since the correlation functions $g(r)$ and $\tilde{g}(r)$ differ only by a constant, the following equality holds:

$$g'(0) = -\frac{O_s}{4}\Delta\varrho^2 \quad (11)$$

Using similar arguments, one can show that the second derivative $g''(r = 0)$ is related to the occurrence of edges. These edges are the boundary lines of the inner surfaces and either are found at a free lateral face of a crystallite or correspond to lines of encounter of two

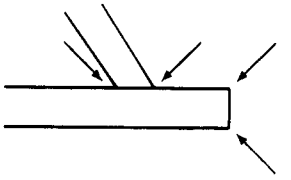

Figure 2. Illustration of the concept of edges on the inner surfaces.

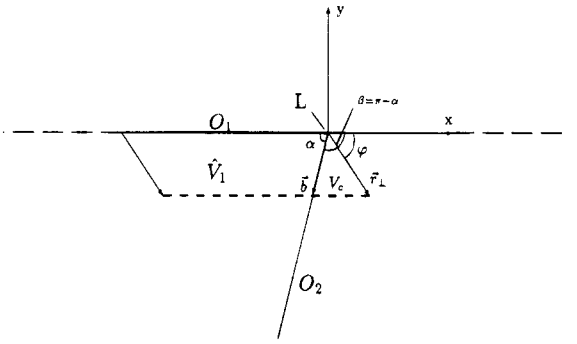

Figure 3. Modification introduced in the geometriacl discussion of the form of $\tilde{g}(r)$, in the case that two surfaces (O_1, O_2) set up an edge.

crystallites. Figure 2 provides a schematic drawing. The relation was first indicated and used in a qualitative way by Mèring and Tchoubar[5,14] and Ramos, Tchoubar, and Pons.[9] A detailed calculation was given by Ciccariello et al.[2,3]. Here we add a simple derivation of the complete expressions which enable a quantitative interpretation of the parameter $g''(0)$. Figure 3 is basically similar to Figure 1 but includes now two interfaces, O_1 and O_2, which enclose an angle α. The crossing line of O_1 and O_2 corresponds to an edge of length L, oriented in the z-direction. Again we are concerned with the determination of the common volume of the shifted and the original structure. If we just use the previous equation (8), $\hat{V}_1(\vec{r})$ is overestimated by the volume V_c depicted in Figure 3 as a triangle. Adding a corresponding correction term and calculating again the isotropic average, we arrive at a modified expression for the correlation function $g(r)$

$$g(r) = g(0) - \frac{O_s}{4}\Delta\varrho^2 r + 2\frac{L_s}{4\pi}\Delta\varrho^2 \int_{4\pi} V_c(\alpha,r,\Omega)\, d\Omega \quad (12)$$

The last term in eq 12 is meant to give only a contribution for $0 \le \varphi \le \beta = \pi - \alpha$, where φ describes the shift direction determined by $\vec{r}_\perp$, the component of $\vec{r}$ perpendicular to the edge. L_s is the "specific length" of the inner edges, i.e., the total length per unit volume of edges at the boundaries of the inner surfaces. Since each edge bounds two inner surfaces, here O_1 and O_2, their effect has to be counted twice, which is accounted for by the factor of 2 in the last term of eq 12. The area V_c can be calculated as

$$V_c = \frac{1}{2}\vec{r}_\perp \times \vec{b} \quad (13)$$

with the vectors

$$\vec{r}_\perp = (r_\perp \cos\varphi, r_\perp \sin\varphi, 0) \quad (14)$$

$$\vec{b} = \left(r_\perp \sin\varphi \frac{\cos\beta}{\sin\beta}, r_\perp \sin\varphi, 0\right) \quad (15)$$

or, since $\beta = \pi - \alpha$, as

$$V_c = \frac{1}{2} r_\perp^2 (\sin\varphi \cos\varphi + \sin^2\varphi \cot\alpha) \quad (16)$$

The isotropic average in eq 12 can be carried out as follows:

$$\frac{L_s}{4\pi}\Delta\varrho^2 \int_0^\pi \sin\theta \, d\theta \int_0^{\pi-\alpha} d\varphi \, r^2 \sin^2\theta (\sin\varphi\cos\varphi + \sin^2\varphi\cot\alpha) = \frac{L_s}{4\pi}\Delta\varrho^2 r^2 \int_0^\pi \sin^3\theta \, d\theta \int_0^{\pi-\alpha} d\varphi \times (\sin\varphi\cos\varphi + \sin^2\varphi\cot\alpha) = \frac{L_s}{4\pi}\Delta\varrho^2 r^2 \frac{4}{3}\left[\frac{1}{2}\sin^2\alpha + \left(\frac{1}{2}(\pi-\alpha) + \frac{1}{4}\sin 2\alpha\right)\cot\alpha\right] = \frac{L_s}{6\pi}\Delta\varrho^2 r^2 [\sin^2\alpha + \sin\alpha\cos\alpha\cot\alpha + (\pi-\alpha)\cot\alpha] \quad (17)$$

The final result for the correlation function $g(r)$ is simply

$$g(r) = g(0) - \frac{O_s}{4}\Delta\varrho^2 r + \frac{L_s}{6\pi}\Delta\varrho^2 r^2 w(\alpha) \quad (18)$$

with a weighting factor $w(\alpha)$ given by

$$w(\alpha) = 1 + (\pi - \alpha)\cot\alpha \quad (19)$$

The weighting factor $w(\alpha)$ is unity for $\alpha = \pi/2$ and vanishes in the limit $\alpha \to \pi$, when the edge disappears. The case $\alpha \to 0$ is irreal, and the divergence for $\alpha \to 0$, therefore irrelevant.

One could suspect at first that any nonplanar, i.e., curved, surface might also give a contribution to $g''(0)$. For a check it is instructive to consider the situation for a spherically curved surface. This case is well-known, as it is analogous to the scattering by a collection of spheres. In the calculation of $g(r)$ here only a third-order contribution, and no second-order contribution in r, shows up.[5] The correlation function $g(r)$ has the following form:

$$g(r) = g(0) - \frac{O_s}{4}\Delta\varrho^2 r + \frac{n_s}{12}\Delta\varrho^2 r^3 \quad (20)$$

where n_s denotes the number of spheres per volume. More general arguments were supplied by Méring and Tchoubar.[5] Indeed, the prerequisite for a contribution to $g''(0)$ is an infinite curvature, as given for an edge.

Derivation of Structure Parameters from the Scattered Intensity. The three parameters $g(0)$, $g'(0)$, and $g''(0)$ can be derived from the scattered intensity $I(s)$. Combining these values with the results of dilatometric measurements, the structural parameters ω, O_s, and L_s and the density difference $\Delta\varrho$ can be obtained.

For $r \to 0$ in eq 1 one obtains immediately

$$g(0) = 4\pi \int_0^\infty ds \, s^2 I(s) = \omega_a \omega_c \Delta\varrho^2 \quad (21)$$

The first derivative $g'(0)$ shows up in the asymptotic behavior of $I(s)$, as given by Porod's law

$$\lim_{s\to\infty} I(s) = -\frac{g'(0)}{2\pi^3 s^4} \quad (22)$$

$$= \frac{P}{s^4} \quad \text{with} \quad P = \frac{O_s \Delta\varrho^2}{8\pi^3} \quad (23)$$

In order to calculate $g''(0)$, we write eq 1 as a sine transformation. Introducing the functions

$$G(r) = rg(r) \qquad J(s) = sI(s) \quad (24)$$

eq 1 transforms into

$$J(s) = 2\int_0^\infty dr \, G(r) \sin(2\pi sr) \quad (25)$$

For the following calculations we need the derivatives of $G(r)$, which are

$$G'(r) = g(r) + rg'(r)$$
$$G''(r) = 2g'(r) + rg''(r)$$
$$G'''(r) = 3g''(r) + rg'''(r) \quad (26)$$

By partial integration of eq 25, we get:

$$J(s) = -2G(r)\frac{\cos(2\pi sr)}{2\pi s}\Big|_0^\infty + 2\int_0^\infty dr \, G'(r)\frac{\cos(2\pi sr)}{2\pi s} = 2G'(r)\frac{\sin(2\pi sr)}{(2\pi s)^2}\Big|_0^\infty - 2\int_0^\infty dr \, G''(r)\frac{\sin(2\pi sr)}{(2\pi s)^2} = 2G''(r)\frac{\cos(2\pi sr)}{(2\pi s)^3}\Big|_0^\infty - 2\int_0^\infty dr \, G'''(r)\frac{\cos(2\pi sr)}{(2\pi s)^3} = -\frac{4g'(0)}{(2\pi s)^3} - 2\int_0^\infty dr \, G'''(r)\frac{\cos(2\pi sr)}{(2\pi s)^3} \quad (27)$$

Using eq 22, we arrive at

$$-8\pi^3 s^4 I(s) - 4g'(0) = 2\int_0^\infty dr \, [3g''(r) + rg'''(r)]\cos(2\pi sr)$$

$$3g''(r) + rg'''(r) = -2\int_0^\infty ds \, [8\pi^3 I(s)\, s^4 + 4g'(0)]\cos(2\pi sr) = -2\int_0^\infty ds \, 8\pi^3 [I(s)\, s^4 - \lim_{s\to\infty} I(s)\, s^4]\cos(2\pi sr) \quad (28)$$

Taking the limit $r \to 0$, we obtain as our final result:

$$g''(0) = \frac{16\pi^3}{3}\int_0^\infty ds \, [\lim_{s\to\infty} I(s)\, s^4 - I(s)\, s^4] = \frac{L_s}{3\pi}\Delta\varrho^2 w(\alpha) \quad (29)$$

In general, we have to assume a distribution of angles α. Then $g''(0)$ gives an average value of the product $\langle L_s w(\alpha)\rangle$.

$$g''(0) = \frac{16\pi^3}{3}\int_0^\infty ds \, [\lim_{s\to\infty} I(s)\, s^4 - I(s)\, s^4] = \frac{1}{3\pi}\langle L_s w(\alpha)\rangle \Delta\varrho^2 \quad (30)$$

Usually scattering data of partially crystalline polymers are analyzed by assuming a one-dimensional model of stacked parallel crystallites and deriving then the one-dimensional interface distribution function or correlation function.[10,12] All contributions of edges are neglected. Obviously, this procedure is only correct if

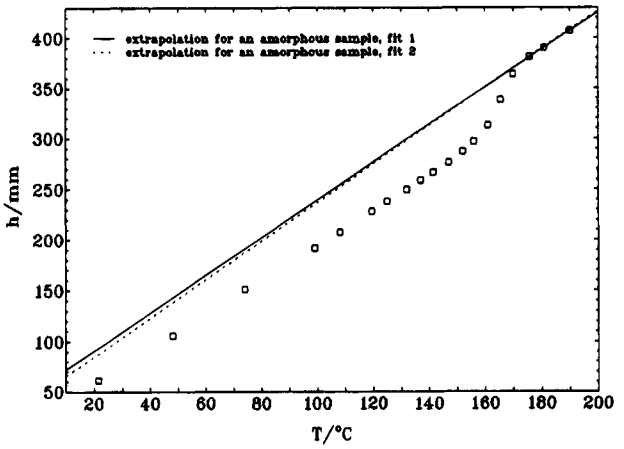

Figure 4. Thermal expansion of PP, as observed in a mercury-filled dilatometer: column height as a function of temperature.

$g''(0) \approx 0$. Equation 29 allows a check and should always be applied before beginning with the data analysis.

Experiments

SAXS experiments were carried out with a conventional X-ray tube and a Kratky compact camera equipped with a temperature-controlled sample holder. The detector system consisted of a scintillation counter and a PC-controlled step system. Using the moving slit method, measurements of absolute intensities were carried out. As the camera is equipped with a slit focus, the data had to be deconvoluted. This was achieved by applying the desmearing algorithm by Strobl.[11]

Sample. The sample material was a commercially available isotactic polypropylene (Hoechst PPN 1060, $M_n = 60\,000$, $M_w/M_n = 2.9$). Samples were molten under vacuum and subsequently isothermally crystallized. For the measurements shown here, the primary crystallization temperature was 160 °C. At such high temperatures PP crystallizes completely in the α-modification. After completion of the primary crystallization, samples exhibit during cooling and reheating temperature-dependent reversible changes in the structure, as reflected in the scattering intensity.

Dilatometry. The small-angle X-ray scattering experiments were complemented by a measurement of the density of the samples. The density at 25 °C was determined by buoyancy measurements. Then the effects of partial melting were monitored using a mercury-filled dilatometer. The measurements were carried out up to temperatures of about 200 °C, heating the dilatometer in an oil bath. Assuming that the amorphous parts in the partially crystalline material have the same density as follows by an extrapolation from the melt, the quantity $\omega_c\Delta\varrho$ can be obtained by subtracting this amorphous density, ϱ_a, from the density ϱ, as determined for the partially crystalline material.

$$\varrho = \varrho_a + \omega_c(\varrho_c - \varrho_a) \tag{31}$$

$$\varrho - \varrho_a = \omega_c\Delta\varrho \tag{32}$$

Figure 4 shows the measured data and the extrapolation described above.

Results

The new concept for an evaluation of SAXS data outlined above found a first application in the study of the temperature-dependent structural changes in isotactic polypropylene. Figure 5 shows a series of SAXS curves obtained at different temperatures during heating. The double-logarithmic representation reveals that

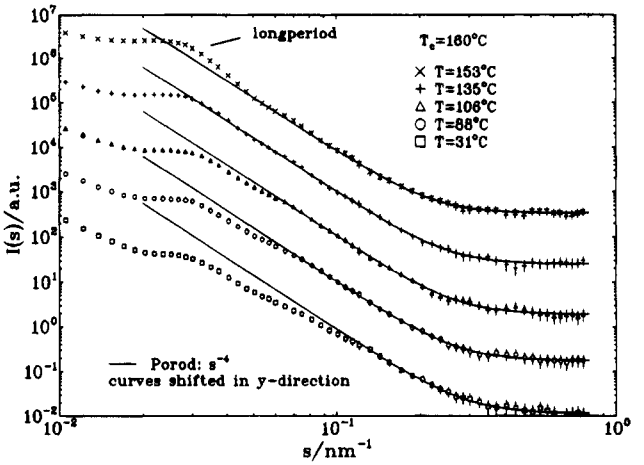

Figure 5. Sample of PP: Scattering intensity $I(s)$ for different temperatures, as observed during heating. The continuous lines give the sum of the Porod contribution and background due to density fluctuations.

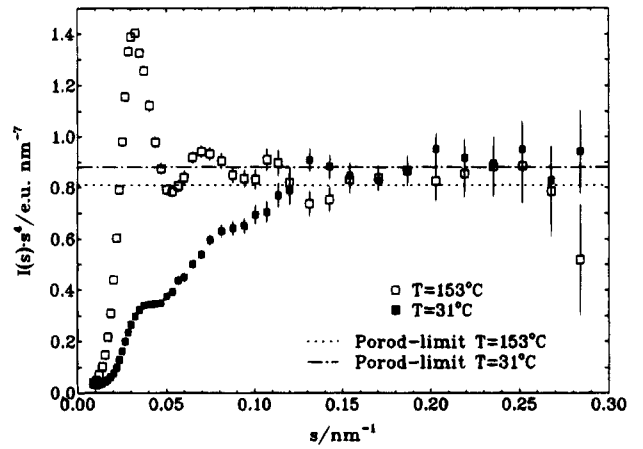

Figure 6. Sample of PP: Scattering intensity $I(s)\,s^4$ for T = 153 and 31 °C, after a substraction of the background scattering due to density fluctuations.

the data agree for high values of s with Porod's law. The continuous line gives the sum of the Porod contribution and a background due to density fluctuations within the single phases, and there is good agreement over a large range in s. Note the absence of any indication for a transition zone between the crystalline and amorphous phase, since this would result in a decay even stronger than Porod's law $I \sim s^{-4}$. For all temperatures a maximum in the intensity at $s \approx 0.03$ nm^{-1} can be seen corresponding to a long period of about 33 nm. The remarkable observation concerns the deviation from Porod's law at lower s: there is a general tendency of $I(s)$ to deviate to lower values, the largest deviations being observed at low temperatures. The lower the temperature the further the scattering curves bend below the extrapolated Porod limit. The integral in eq 30 and therefore the parameter $g''(0)$ depend exactly on these deviations, and we may conclude that $g''(0)$ increases with decreasing temperature. Figure 6 shows two selected curves in a plot of the product $I(s)\,s^4$ versus the scattering vector s, the contribution due to the density fluctuations being subtracted. The deviation from Porod's law of the curve observed at 31 °C is obvious. Hence, recalling the implications of a nonvanishing value of $g''(0)$, we have evidence that edges form on lowering the temperature below the original crystallization temperature. Since the long period remains

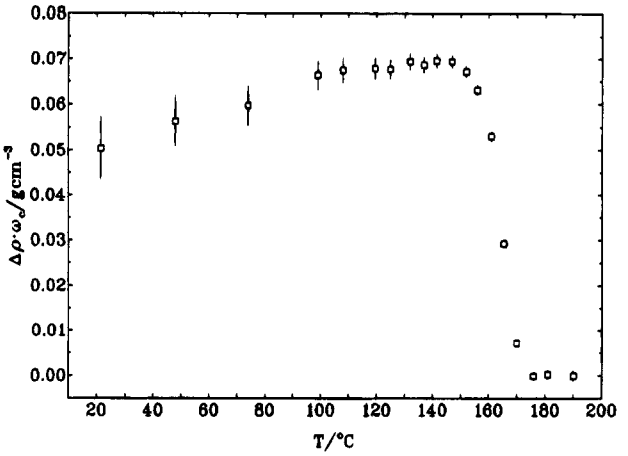

Figure 7. Sample of PP, product $\omega_c\Delta\varrho$ as a function of temperature, as measured by dilatometry, T_c = 160 °C.

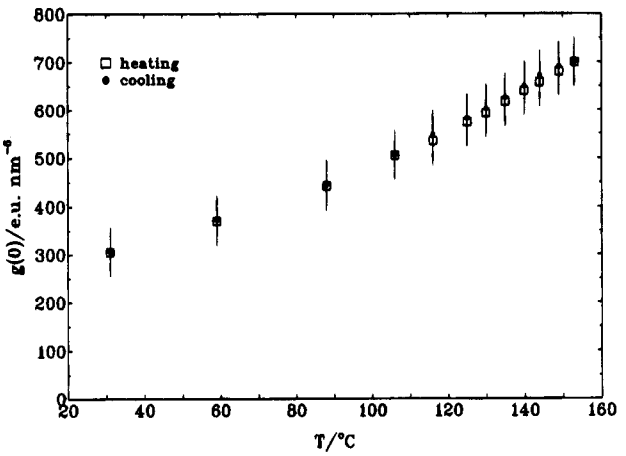

Figure 8. Sample of PP: Invariant $g(0)$ as a function of temperature, T_c = 160 °C.

unchanged, formation of new small crystallites in the amorphous regions, which have oblique orientations, is suggested.

This first qualitative analysis of the scattering data is further confirmed by a quantitative analysis based upon the three parameters $g(0)$, $g'(0)$, and $g''(0)$, in combination with dilatometry. The usual analysis in terms of the one-dimensional correlation function or the derived interface distribution function is not applicable here, because this requires a vanishing value of $g''(0)$. Only at the highest temperature does this condition appear to be fulfilled.

The combination of small-angle X-ray scattering and dilatometry was possible, since the dilatometric measurements were performed directly after the SAXS experiments on the same sample avoiding a new primary crystallization. Figure 7 shows the values of $\omega_c\Delta\varrho$, as derived from the dilatometric data in Figure 4. Errors result mainly from the uncertainty in ϱ_a, obtained by an extrapolation from the melt. Due to the high melting temperature of polypropylene, measurements on the melt could only be performed in a fairly small temperature range. The two lines in Figure 4 represent bounds for possible extrapolations. Figures 8–10 show the parameters $g(0)$, P, and $g''(0)$ as derived from the SAXS data. Values obtained during cooling and heating the sample are given for comparison. The temperature-dependent changes are practically reversible. The error in the determination of the invariant $g(0)$ is mainly caused by the uncertainty in the extrapo-

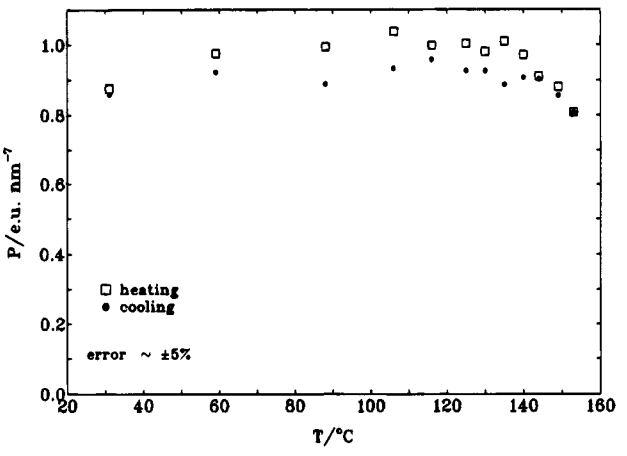

Figure 9. Sample of PP: Porod parameter P as a function of temperature, T_c = 160 °C.

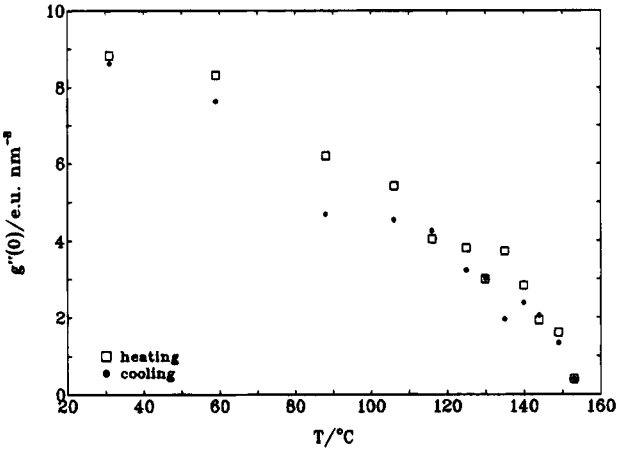

Figure 10. Sample of PP: $g''(0)$ as a function of temperature, T_c = 160 °C.

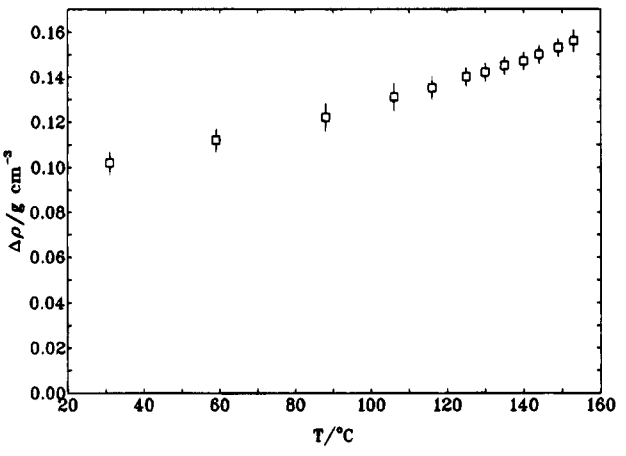

Figure 11. Sample of PP: density difference $\Delta\varrho$ as a function of temperature.

lation of the function $I(s)\,s^2$ for $s \to 0$, which is required for a calculation of the integral

$$g(0) = 4\pi\int_0^\infty ds\; s^2 I(s)$$

At very small angles we observed an additional parasitic scattering, which had to be subtracted by empirical means. The total error may amount to 10% of $g(0)$.

In Figures 11–14 the results of the quantitative data evaluation are shown. The difference in density between the amorphous and the crystalline phase amounts

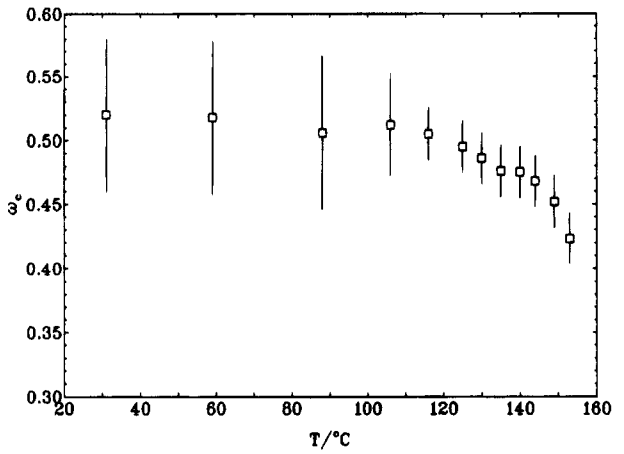

Figure 12. Sample of PP: Crystallinity ω_c as a function of temperature, as observed during heating, T_c = 160 °C.

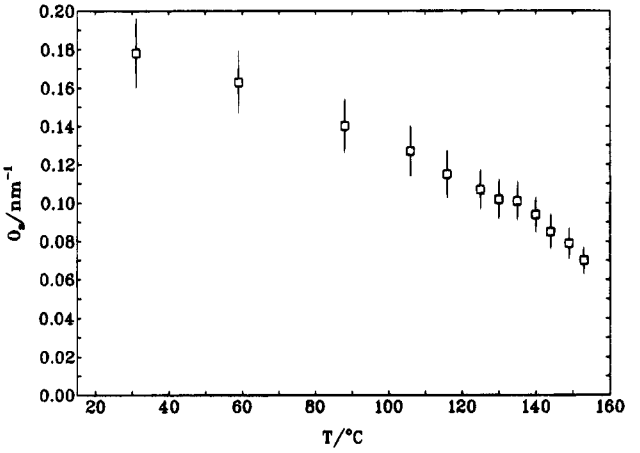

Figure 13. Sample of PP: Specific inner surface O_s as a function of temperature, as observed during heating, T_c = 160 °C.

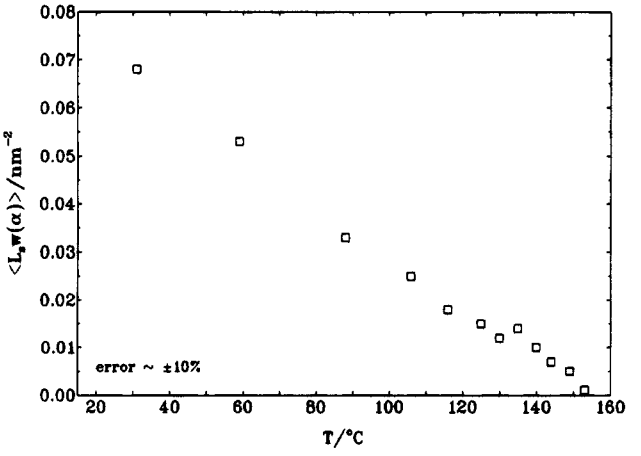

Figure 14. Sample of PP: Specific length of edges $\langle w(\alpha)\, L_s \rangle$ as a function of temperature, as observed during heating, T_c = 160 °C.

at 31 °C to $\Delta\varrho = 0.102 \pm 0.005$ g cm^{-3}. This is slightly higher than the values published by other authors ($\Delta\varrho$ = 0.093–0.095 g cm^{-3} [15]). Using this result the other structure parameters can be determined. The crystallinity after the primary crystallization is $\omega_c \approx 0.5$; lowering of the temperature then leads to an increase. The large error bars at low temperatures originate from the uncertainty in $\omega_c \Delta\varrho$. Accurate results are obtained for the specific inner surface O_s and the specific length of edges L_s. A decrease in temperature below the original crystallization temperature leads to a strong increase for both parameters. At the highest temperature, T = 153 °C, the relation

$$L = 2/O_s$$

which is valid for the regular one-dimensional stack model, approximately holds:

$$L = 33 \pm 0.5 \text{ nm} \qquad 2/O_s = 29 \pm 2.5 \text{ nm}$$

At low temperatures a large discrepancy is noted

$$L\frac{O_s}{2} \approx 2.5$$

confirming again that we are no longer dealing with a one-dimensional stack.

Completely analogous results have been obtained in experiments with a lower temperature of primary crystallization, T_c = 140 °C, and also with other samples (Moplen D50G from Himont).

Conclusions

The results obtained from small-angle X-ray scattering demonstrate that the amorphous–crystalline structure in polypropylene changes with temperature. After completion of the primary crystallization, additional crystallization takes place on cooling the sample.

Analysis of the data first indicates that the one-dimensional model becomes inappropriate when considering the structural changes during cooling. Only the primary crystallization at high temperatures results in a structure, which can be described as a stack of crystalline lamellae. The changes in the scattering on cooling lead to a nonvanishing $g''(0)$, thus violating the conditions under which a one-dimensional model can be applied. The observed increase of $g''(0)$ is indicative of a growing number of edges, located at the boundaries of newly formed crystallites. These additional crystallites develop in the existing amorphous layers, resulting in an increase both of the inner surface O_s and of the length L_s of edges. The additional crystallites must be much smaller than the primary laterally extended lamellae, since they leave the long period unchanged. A rough estimate of the size of the additional crystallites can be derived from the ratio between the additional interface and the length of edges associated with the formation of the crystallites. The ratio yields a characteristic length, l.

$$l = \frac{O_s(T) - O_s(153\ ^\circ\text{C})}{\langle w(\alpha)\, L_s(T) \rangle} \tag{33}$$

As we may associate the edges with lateral bounds of the crystallites, l indicates the order of magnitude of the crystallite diameter. Figure 15 shows l as a function of temperature. Values are indicative for crystallites with a size of a few nanometers. They would be indeed small enough to be incorporated into those layers, which after the primary crystallization remained at first amorphous (their thickness is $L(1 - \omega) \approx 17$ nm). As expected, the crystallites get even smaller at higher undercoolings.

We assume that this peculiar mode of partial crystallization is related to the special cross-hatched morphology of isotactic polypropylene, as observed by electron

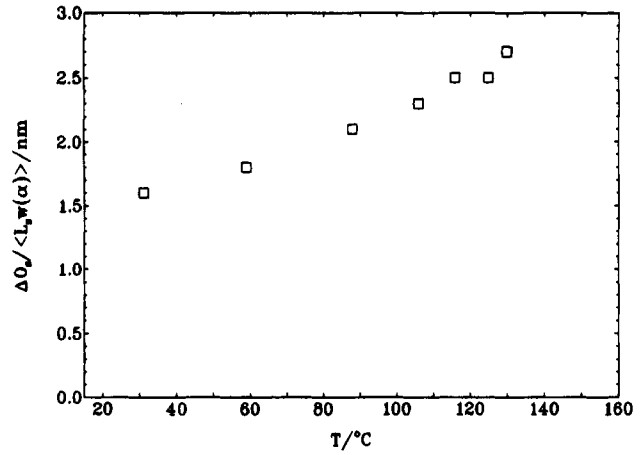

Figure 15. Sample of PP: Estimated typical size of crystals formed by the additional crystallization below T_c, T_c = 160 °C.

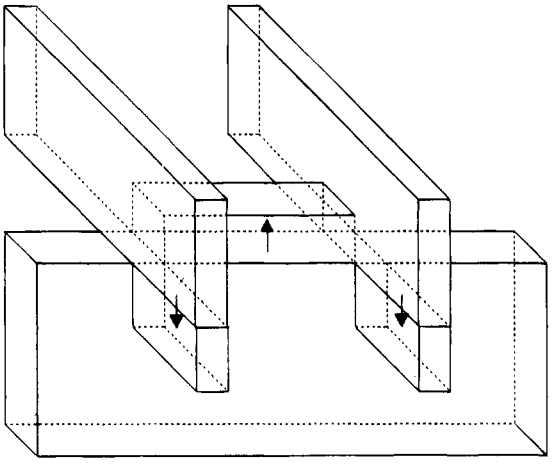

Figure 16. Model suggested for the process of partial crystallization and melting in isotactic polypropylene.

microscopy. Studies revealed the simultaneous occurrence of lamellae oriented nearly perpendicular to each other. Lotz and Wittman[4] explained these findings by an epitaxial mode of crystallization, leading to a structure as sketched in Figure 16. On the basis of this model, it may now be suggested that the observed generation of additional interface area and edges results from a further growth of the lamellae near the contact points in a direction as indicated by the arrows in Figure 16. On lowering the temperature, the additional crystallization advances further into the amorphous regions. On heating the sample the reverse process takes place. The suggested model thus combines the new findings of the SAXS experiments with previous knowledge obtained by electron microscopy.

Acknowledgment. We thank S. Stückler for assistance in the dilatometric measurements. Support of this work by the Deutsche Forschungsgemeinschaft (SFB 60, Freiburg) is gratefully acknowledged.

References and Notes

(1) Bassett, D. C.; Olley, R. H. *Polymer* **1984**, *25*, 935.
(2) Ciccariello, S.; Cocco, G.; Benedetti, A.; Enzo, S. *Phys. Rev. B* **1981**, *23*, 6474.
(3) Ciccariello, S.; Benedetti, A. *Phys. Rev. B* **1982**, *26*, 6384.
(4) Lotz, B.; Wittmann, J. C. *J. Polym. Sci., Polym. Phys. Ed.* **1986**, *24*, 1541.
(5) Méring, J.; Tchoubar, D. *J. Appl. Crystallogr.* **1968**, *1*, 153.
(6) Norton, D. R.; Keller, A. *Polymer* **1985**, *26*, 704.
(7) Olley, R. H.; Bassett, D. C. *Polymer* **1989**, *30*, 399.
(8) Porod, G. In *Small Angle X-ray Scattering*; Glatter, O., Kratky, O., Eds.; Academic Press: London, 1982.
(9) Ramos, A.; Tchoubar, D.; Pons, C. H. *J. Phys. IV* **1993**, *C8* (3), 377.
(10) Ruland, W. *Colloid Polym. Sci.* **1977**, *255*, 417.
(11) Strobl, G. R. *Acta Crystallogr.* **1970**, *A26*, 367.
(12) Strobl, G. R.; Schneider, M. *J. Polym. Sci.* **1980**, *18*, 1343.
(13) Tanabe, Y.; Strobl, G. R.; Fischer, E. W. *Polymer* **1986**, *27*, 1147.
(14) Tchoubar, D.; Méring, J. *J. Appl. Crystallogr.* **1969**, *2*, 128.
(15) Wunderlich, B. Crystal Melting. *Macromolecular Physics*; Academic Press: New York, 1980; Vol. 3.

MA9500906